Journal of The Electrochemical Society, **154** (9) D482-D488 (2007)
0013-4651/2007/154(9)/D482/7/$20.00 © The Electrochemical Society

A Comparison of Chemical Bath Deposition of CdS from a Batch Reactor and a Continuous-Flow Microreactor

P. H. Mugdur,[a] Y.-J. Chang,[a,*] S-.Y. Han,[a,b] Y-W. Su,[a] A. A. Morrone,[c] S. O. Ryu,[a,b] T.-J. Lee,[b] and C.-H. Chang[a,,z]**

[a]*Department of Chemical Engineering, Oregon State University, Corvallis, Oregon 97331, USA*
[b]*School of Chemical Engineering and Technology, Yeungnam University, Kyongsan 712-749, South Korea*
[c]*Seagate Technology, Minneapolis, Minnesota 55435-5489, USA*

In this paper, we report a comparison between CdS deposition by a conventional batch reactor and a newly developed continuous-flow microreactor. This microreactor setup makes use of a micromixer for efficient mixing of the reactant streams and helps in controlling the homogeneous reaction before the solution impinges on a substrate. Transmission electron microscopy analysis indicated that an impinging flux without the formation of nanoparticles could be obtained from this reactor at a short residence time. The surface morphology of the deposited films clearly indicated an improvement of film smoothness and coverage over films deposited from a batch process. Highly oriented nanocrystalline CdS films were obtained from the continuous-flow microreactor in contrast to poor crystalline films from the batch process. This new approach could be adopted for the deposition of other compound semiconductor thin films at low temperatures using a solution-based chemistry with improved control over the processing chemistry.
 [DOI: 10.1149/1.2757012]

Manuscript submitted November 13, 2006; revised manuscript received April 30, 2007. Available electronically July 27, 2007.

Metal chalcogenide compound semiconductors have received much attention for electronic and optoelectronic applications. Typically, metal chalcogenides were deposited as binary or ternary compounds including sulfide, selenide, and telluride[1-3] using a variety of techniques such as electrodeposition,[4] vacuum evaporation,[5] successive ionic-layer adsorption and reaction (SILAR),[6] spray pyrolysis,[7] sputtering,[8] chemical vapor deposition (CVD),[9] and chemical bath deposition (CBD).[10-12] Among these, CBD is attractive due to its low temperature, low cost, and large-area-deposition capability. Many chalcogenide semiconductors have been successfully deposited using this technique and it has already proven to be a very useful method for fabricating large-area devices such as high-efficiency $CuInSe_2$ and CdTe solar cells.[13,14]

Though CBD has many advantages, it suffers from some drawbacks. In the case of a batch-CBD process, the heat needed for chemical reaction is supplied from the solution bath to the sample surface, resulting in both heterogeneous CdS nucleation at the surface as well as homogeneous CdS formation in the bath. Hence, for baths involving a thermal jacket (glass beaker, etc.) or water bath, significant CdS deposition also occurs on the walls of the vessels. In addition, the bath should be stirred continuously to ensure uniform thermal and chemical mixing and to minimize sticking of homogeneously nucleated CdS particles to the growing film surface. Moreover, the unequal volume of the bath used to form the desired CdS film generates a lot of waste and creates defects in devices. Although efforts have been made by various group of researchers to reduce the bath-to-surface volume with the use of cover plates,[15] a comprehensible path for combining large-area deposition with high utilization and growth rate for high-conversion efficiencies has not yet been demonstrated.

Recently, we have developed a continuous flow microreactor (CFM) to overcome the drawbacks associated with a typical batch-CBD process.[10] This novel microreactor setup makes use of a micromixer for efficient mixing of the reactant streams and helps to control the homogeneous reaction before the solution impinges on a substrate. Uniform, smooth, and highly oriented nanocrystalline CdS semiconductor thin films were successfully deposited on oxidized silicon substrates at low temperatures using this microreactor. Furthermore, functional thin-film transistors were fabricated from the as-deposited films without any postannealing process.[10] In this paper, we report a comparison between the CdS films deposited by a conventional batch reactor and this newly developed CFM.

Experimental

Oxidized silicon substrates (silicon wafer coupons) measuring 15×10 mm were used for deposition studies. The coupons were initially sonicated in an ultrasonic bath using 1 M NaOH for about 10–15 min and then cleaned according to a standard acetone, methanol, and deionized (DI) water (AMD) procedure. Finally, they were dried under a stream of nitrogen gas before being used for deposition.

CBD-batch reactor consists of an 800 mL glass beaker mounted on top of a VWR hot plate stirrer. The substrates were taped to a 75×25 mm microscope glass slide after cleaning by the AMD procedure and immersed in a beaker filled with 436 mL of Millipore DI water. 60 mL of 0.44 g $CdCl_2$ and 20 mL of 1.28 g NH_4Cl were added slowly with a stirring rate of 200 rpm and the temperature of the reaction mixture was monitored using a thermometer. When the temperature reached 80°C, 60 mL of 1.86 g thiourea was added and the addition of thiourea decreased the temperature to around 70°C. The heating was continued until the reaction mixture reached 80°C again, and 24 mL (28–30 wt %) NH_4OH was added at this time to begin the reaction (~75°C) with the pH value ~11. The final concentration of the reactants were 0.004 M $CdCl_2$, 0.04 M NH_4Cl, 0.04 M thiourea, and 0.4 M NH_4OH with a total solution volume of 600 mL. The reaction was allowed to proceed for a defined period of time and then the substrates were taken out of the solution, removed from the glass slide, washed with DI water, and dried under a stream of nitrogen.

The CFM used in our experiments basically consists of two 25 mL syringe pumps and a micromixer. They were connected using polyetheretherketone (PEEK) tubes [1/16 in. outside diameter (o.d.), 0.03 in. inside diameter (i.d.) from Upchurch Scientific] as shown in Fig. 1. Two syringe pumps (V6 module from Kloehn Ltd.) were used, for holding reactant streams 1 and 2 before mixing. Each pump has three ports (A, B, and C). One port of each pump was used for aspirating the reactant streams and the other port was used for dispensing them. The standard slit interdigital micromixer (SSIMM from Institut fur Mikrotechnik Mainz, Germany)[16] was used for our experimental studies. It is essentially made of stainless steel (SS) 316Ti housing with an inlay of thermally oxidized silicon (30×100 μm channels). These mixer inlays are fabricated by advanced silicon etching (ASE) technique. For all experiments, reactant streams 1 and 2 were initially pumped into syringes and then dispensed through the PEEK tube and allowed to mix in the micro-

* Electrochemical Society Student Member.
** Electrochemical Society Active Member.
z E-mail: changch@engr.orst.edu

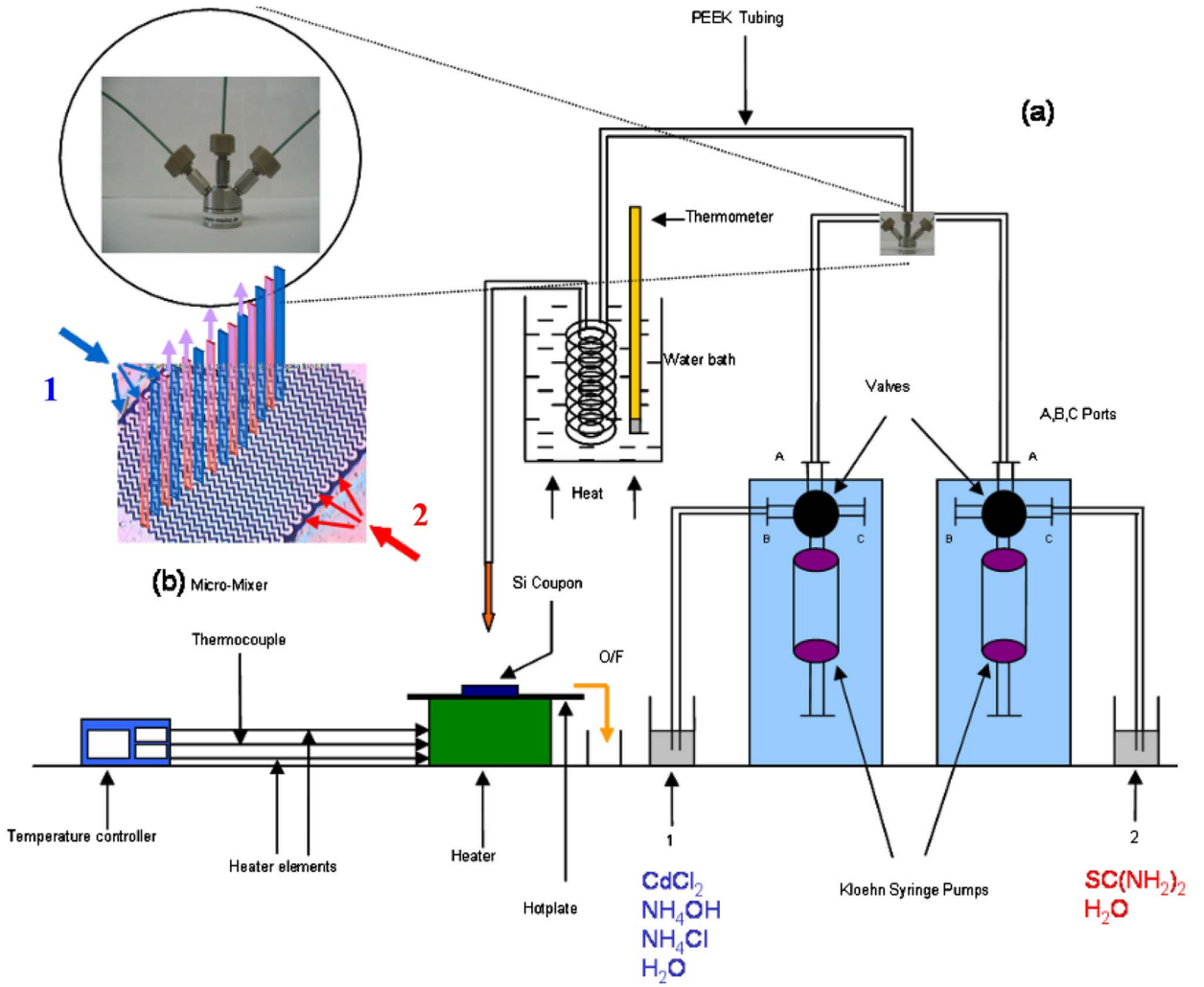

Figure 1. (Color online) Schematic diagram of (a) a CFM experimental setup and (b) an interdigital micromixer.

mixer. Stream 1 consists of 12 mL of 0.036 g $CdCl_2$, 10 mL of 0.105 g NH_4Cl, and 2 mL of (28–30 wt % NH_4OH, where stream 2 consists of 12 mL of 0.15 g thiourea and 13 mL of DI water. The overall final concentration of the reactants were 0.004 M $CdCl_2$, 0.04 M NH_4C1, 0.04 M thiourea, and 0.4 M NH_4OH, the same as the concentrations used in the CBD batch reaction. The resulting mixture was passed through a 5 ft long coil (PEEK), which was immersed in a hot water bath maintained at 80–85°C. The solution impinged on the substrate, which was taped to a 3 in. diameter SS metallic plate and heated on a hot plate (2 in. diameter × 0.75 in. thick SS disk from Watlow) at 80–90°C.The syringe pumps were operated at a speed of 250 steps/s (Hz) corresponding to the flow rate of ~0.13 mL/s and the mean residence time of the mixture after passing the micromixer and emerging from the PEEK tube was about 3 s. The deposition time is limited to 3.12 min by the capacity of the syringe pumps (25 mL) used for this study. A deposition rate around 400 Å/min was determined by the surface profiler. Once the process was completed, the substrate was removed from the plate, washed with Millipore DI water, and dried under a stream of nitrogen gas.

The CdS thin-film morphology was characterized by scanning electron microscopy (SEM, Hitachi S-4100 FE-SEM) with a cold field-emission electron gun and AFM (DI Nanoscope III) in contact mode. For the particle formation study, transmission electron microscopy (TEM) (JEOL 2010 TEM operated at 200 kV) was used along with selected area electron diffraction (SAED) and energy dispersive X-ray (EDX) analysis. In the preparation of TEM samples for both batch reactor and CFM, the copper grids (with thin lacey carbon films) were dipped in a hot solution collected from reactors at a certain reaction time for about 10 s. The phase and crystalline orientation was determined by X-ray diffraction (XRD) using a diffractometer (D8 Discover, Bruker) with a Cu Kα1 source. Thicker films (~500 nm) were used for XRD analysis to obtain a better signal. For the batch process, the silicon substrate was deposited for 3.12 min and taken out with water rinsing. This process was repeated seven times to get a final film thickness around 500 nm. The same thickness of CdS films was obtained from the continuous-flow microreactor by repeating the deposition four times. XPS analysis (VG ESCALAB 220-IXL instrument with Mg Kα radiation) was used to characterize the chemistry for the deposited thin films on silicon coupons.

The optical absorption and transmission spectra of the CdS thin films were measured by a UV-visible spectrophotometer (Ocean Optics Inc. USB 2000 optic spectrometer) to obtain the estimated optical bandgap from both deposition methods.

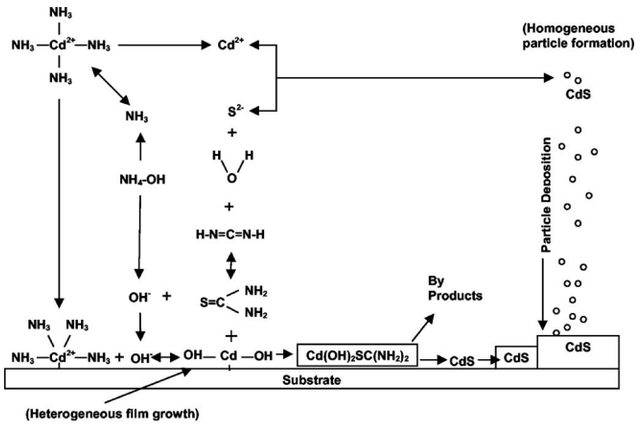

Figure 2. Schematic diagram of CBD-CdS growth mechanisms.

Results and Discussion

The fundamental aspects of CBD are similar to those of a CVD process. It involves mass transport of reactants, adsorption, surface diffusion, reaction, desorption, nucleation, and growth. Earlier studies[17] suggested a colloidal-by-colloidal growth model. However, more recent investigations by Ortega-Borges and Lincot[18] suggested a different growth kinetics based on initial rate studies using a quartz crystal microbalance (QCM). They identified three growth regimes: an induction period with no growth observed, a linear growth period, and finally a colloidal growth period, followed by the depletion of reactants. They proposed a molecular-level heterogeneous reaction mechanism given in Eq. 1-3

$$Cd(NH_3)_4^{2+} + 2OH^- + \text{site} \underset{k_{-1}}{\overset{k_1}{\rightleftarrows}} Cd(OH)_{2\ ads} + 4NH_3 \qquad [1]$$

$$Cd(OH)_{2\ ads} + SC(NH_2)_2 \overset{k_2}{\rightarrow} \{Cd[SC(NH_2)_2](OH)_2\}_{ads} \qquad [2]$$

$$\{Cd[SC(NH_2)_2](OH)_2\}_{ads} \overset{k_3}{\rightarrow} CdS + CN_2H_2 + 2H_2O + \text{site} \qquad [3]$$

This model has provided a good understanding of the CBD process at the molecular level. It is well known that particle formation plays an important role in the CBD process. Kostoglou et al.[19] reported a detailed and comprehensive model for the CBD CdS process. This model includes the particle nucleation, growth, and deposition in addition to the molecule-by-molecule film growth. A schematic diagram that illustrates both homogeneous and heterogeneous reaction is given in Fig. 2. We have observed that small particles were forming and growing even at the beginning of the process through dynamic light scattering and TEM measurements.[12] These experimental results indicated the importance of particle formation even in the linear-growth regime. It is necessary to find a method to decouple the homogeneous particle formation and deposition from the molecular-level heterogeneous surface reaction for better understanding and optimization of the CBD process.

Our CFM was developed for this purpose. The continuous-flow microreactor illustrated in Fig. 1 includes an interdigital micromixer. Micromixers offer features which cannot be easily achieved by macroscopic devices, such as ultrafast mixing on microscale.[20] A detailed schematic diagram of an interdigital micromixer is shown in Fig. 1b. Solutions 1 and 2 to be mixed are introduced into the mixing element as two counterflows and enter interdigital channels (30 μm) and split into many interpenetrated substreams. The substreams left in the interdigital channel are perpendicular to the direction of the feed flows, initially with a multilayered structure. Fast mixing through diffusion follows due to the small thickness of the individual layer. The resulting mixture from the micromixer was passed through a 5 ft long a coil (PEEK) immersed in a hot-water bath maintained at 80–85°C (using a VWR hot plate stirrer). The homogeneous chemistry of the impinging flux could be controlled by the length of the microchannel, flow rate, and the residence time.

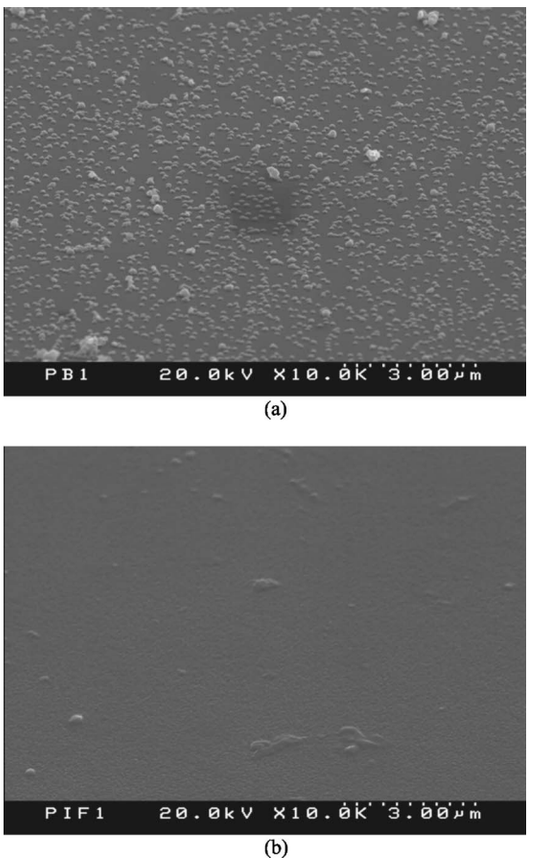

Figure 3. SEM images of CdS films deposited by (a) a batch reactor and (b) a CFM.

Figure 3 shows the SEM images of CdS films deposited by (a) a batch reactor and (b) a CFM. It can be clearly seen from the SEM that the film deposited by the continuous-flow microreactor is smooth and continuous, while the batch reactor produced isolated CdS dots on the order of hundreds of nanometer. Figure 4 compares 2×2 μm AFM scans of CBD CdS films deposited on silicon-oxidized substrate using the batch and the continuous-flow microreactor processes. These AFM images show a clear difference in the appearance of the surface for samples deposited by the batch and the continuous-flow microreactor. Figure 4a shows the surface morphology of the deposited CdS on an oxidized silicon substrate using a batch reactor for 3.12 min. The AFM image shows either the isolated or groups of pyramid-shaped CdS nanocrystals grown on top of the oxidized silicon substrate. The sample has a root-mean-square (rms) surface roughness of 19.592 nm with a mean roughness of 15.795 nm. Figure 4b shows the surface morphology of the deposited film of the same scan size (2×2 μm) in the continuous-flow microreactor. The AFM image shows that a continuous nanocrystalline film was formed in the continuous process while the discontinuous CdS nanocrystals were produced in the batch process after the same deposition time. The rms value of roughness was found to be 11.751 nm with a mean roughness of 9.606 nm. The reactant concentration of the batch process decreased quickly as the reaction proceeded due to homogeneous particle formation.[12] In contrast, the CFM supplied a reactant flux with constant concentration that pro-

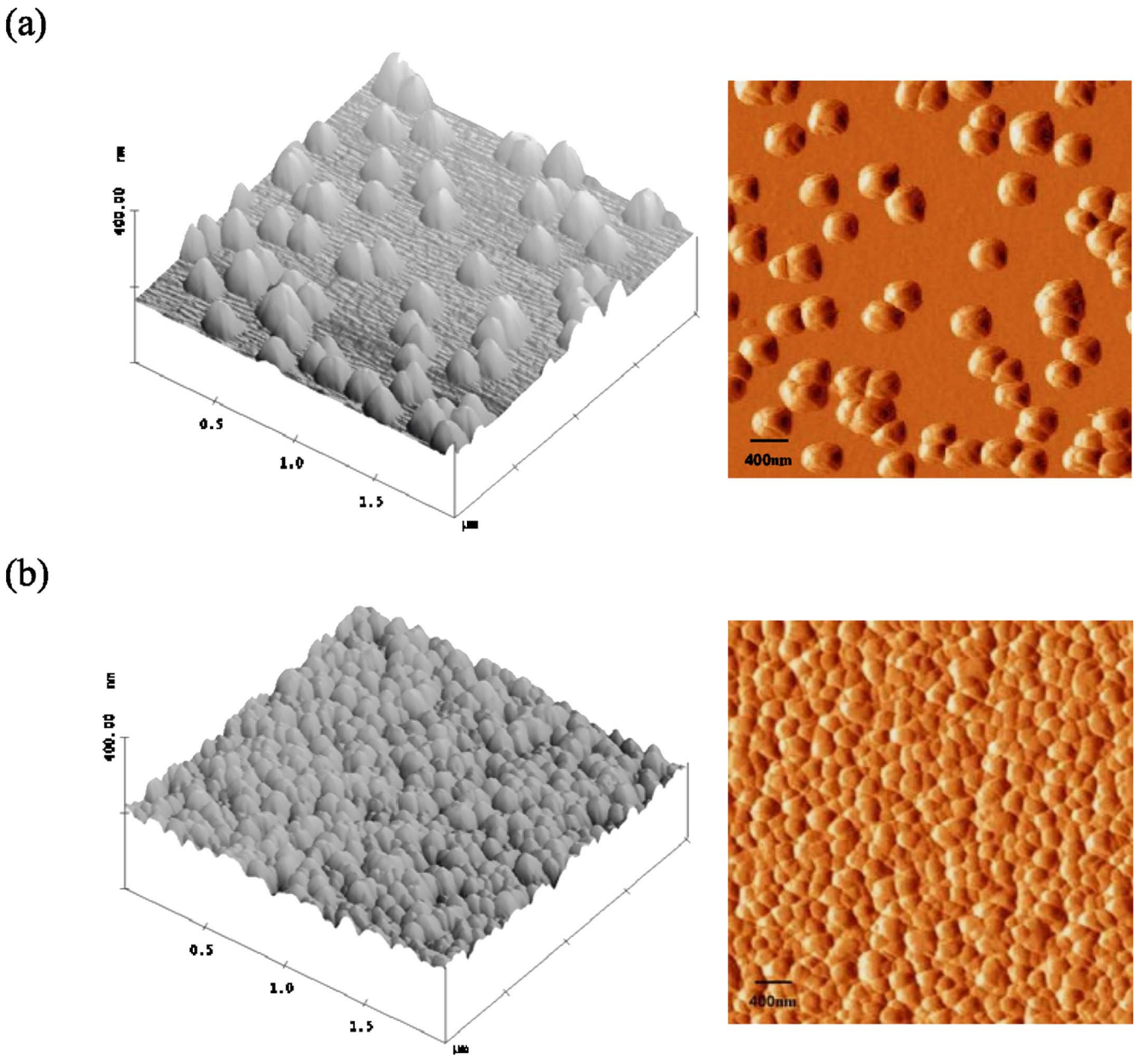

Figure 4. (Color online) AFM images of CdS films deposited by (a) a batch reactor and (b) a CFM.

vides a higher nucleation density. This higher nucleation density made a significant difference in film coverage between the batch and the continuous-flow microreacter process.

A thin film (about 5000 Å) of CdS was deposited on a silicon coupon with the CFM in the temperature range of 85–90°C and it was characterized by XRD. Figure 5a is a typical X-ray diffractogram which shows diffraction peaks at $2\theta = 26.5$ and 55°. These diffractogram peaks were compared with the standards in the JCPDS data files.[21] The as-deposited material appears to be composed of the cubic phase of CdS. In particular, the sharp peak at 26.5° corresponds to the (111) Bragg reflection planes from the cubic (zincblende) phase (the possibility of hexagonal phase could not be ruled out completely). It is indicated that the film is strongly oriented along (111) with another small peak at (222) orientation. The presence of only (111) and (222) peaks indicates the highly oriented nature of CdS films deposited by the CFM which must grow as successive alternative planes composed of only either Cd or S atoms parallel to the substrate surface, as it corresponds to the (111) planes of the cubic crystalline structure. This type of growth is in good agreement with the molecular-level growth mechanism. In contrast, the XRD spectrum from the batch process shows peaks from (111), (200), (220), and (311) planes. The intensity of the peaks is much lower than the peaks from the films deposited by the CFM. This result indicates that the films deposited by the batch process were more randomly oriented and had lower crystallinity.

To further study the difference between the batch and the continuous-flow processes, we analyzed the solution by TEM, SAED, and EDX. Figure 6 shows the TEM micrographs of CdS particles obtained by dipping the copper grids covered by thin lacey carbon films for 10 s in a batch-reactor solution at 80°C when the reaction time t was 3.12 min. We can see many agglomerates like bunches of grapes with particles over 0.1 μm in size shown in Fig. 6a. Each of these agglomerates contains a number of crystalline nanoparticles of the order of 10 nm in diameter each.

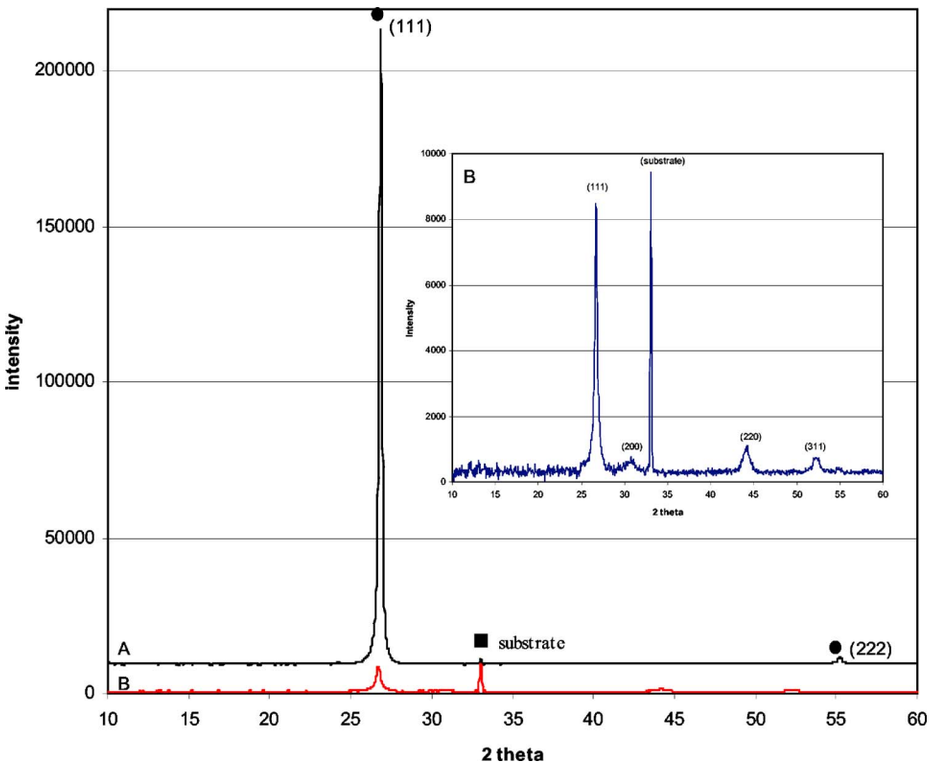

Figure 5. (Color online) X-ray diffractogram of CdS film deposited by (a) a CFM and (b) a batch reactor.

The corresponding SAED pattern is given in Fig. 7a. The observed lattice-plane spacing-d values are in good agreement with the JCPDS power diffraction data for the cubic phase of CdS as shown in Fig. 7a. Also, the experimental lattice constant, a = 5.87 Å, is in good agreement with the literature value of 5.82 Å for cubic CdS phase.

In the EDX spectrum, the peaks of Cd and S are pronounced with a Cd/S ratio of 43.1:56.9 atom % as shown in Fig. 7b. The presence of Cl peak is due to the reagents $CdCl_2$ or NH_4Cl used in the CBD process and the Cu peak can be attributed to copper grids used in the sample-preparation process.

Similarly, TEM samples were also obtained by dipping copper grids (with thin lacey carbon film) in hot solution, collected from the CFM, for about 10 s. There was no evidence of any particles on the surface of the grid as shown in Fig. 8. This sample had no crystallinity and nothing of interest was found. Also, the EDX did not show any CdS. This result indicates that the impinging reactant flux from the CFM is particle free under this operating condition. Thus, the CdS films were grown through a molecule-by-molecule mechanism.

The absorption measurement of the as-deposited CdS thin film, measured at various wavelengths by a UV-visible spectrophotometer, was used to estimate the optical bandgap. Two plots of $(\alpha E)^2$ vs E for thin film deposited on a glass slide by a batch reactor and a CFM are shown in Fig. 9a and b, respectively. Extrapolation of the linear portion of the curve to $(\alpha E)^2 = 0$ gives the estimated optical bandgap of 2.41 eV from a batch reactor and 2.43 eV from a CFM. Both values are in good agreement with the reported bandgap value of 2.42 eV for CdS.[22,23]

The as-deposited CdS layers deposited by batch reactor and CFM were analyzed by XPS. The XPS spectra for our CBD CdS were typical of CdS films reported by other researchers.[24,25] The results are shown in Fig. 10 and summarized in Table I. For batch CdS films, the binding energies of Cd $3d_{5/2}$ and Cd $3d_{3/2}$ at ~405.2 and ~411.9 eV and that of S 2p at ~161.7 eV for the films were indicative of the CdS chemistry. We observed the presence of carbon and oxygen as impurities in the as-deposited films. The carbon peak present in these samples, is present as an impurity in all the samples

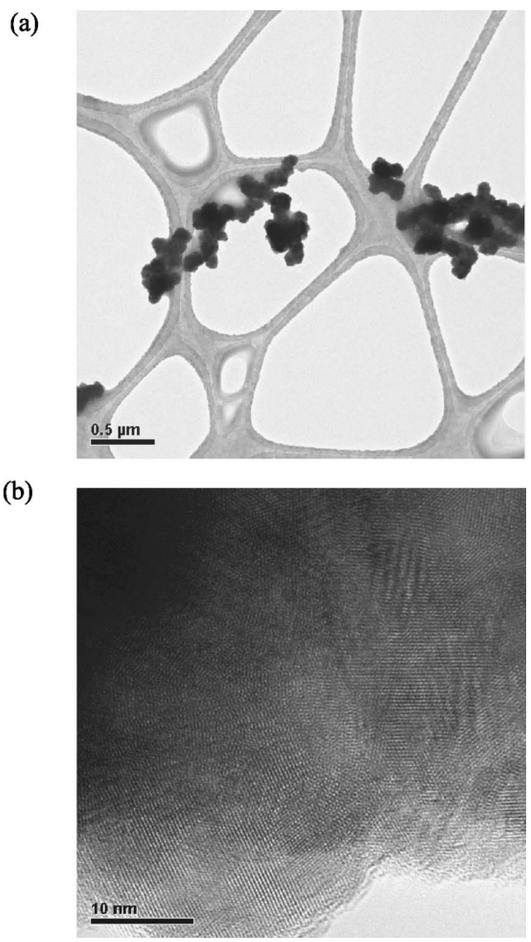

Figure 6. TEM micrographs of CdS particles produced from a batch reactor: (a) low resolution and (b) high resolution.

(a)

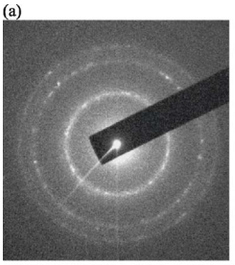

Observed d-spacing values (Å)	JCPDS 80-0019 (Cubic CdS)
3.36	3.35 (111)
	2.91 (200)
2.07	2.05 (220)
1.77	1.75 (113)
	1.68 (222)
	1.45 (400)
1.35	1.33 (331)
	1.29 (420)

(b)

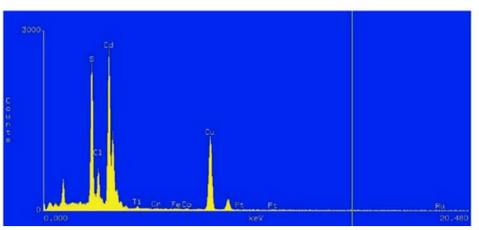

Figure 7. (Color online) (a) SAED pattern and (b) EDX spectrum of CdS particles from the batch reactor.

exposed to atmosphere. The energy scale was calibrated using this carbon peak (C 1s at 284.2 eV) as a reference. The Si 2p peak in the batch-produced film at binding energy of 103.2 eV suggests SiO_2 and is most likely due to the incomplete coverage of CdS films.

Conclusion

We have developed a continuous-flow microreactor for the CBD process.[10] In this paper, we reported a comparison between CdS deposition by a conventional batch CBD reactor and deposition by a CFM. The CFM makes use of an interdigital micromixer to achieve efficient mixing of the reactant streams in a short time. This novel reactor provides an advantage of introducing constant flux of reactant solutions to the system (continuous process) that allows control over the homogeneous reaction of the chemical bath solution before the solution impinges on the substrate. We have successfully created a reactant flux that is particle free by controlling the residence time.

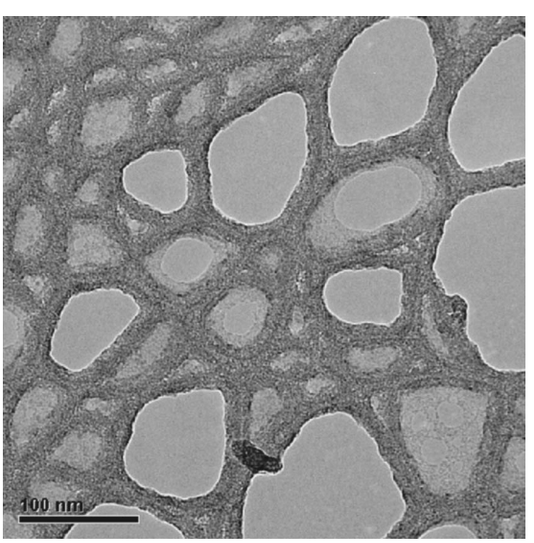

Figure 8. TEM image showing the absence of CdS particles from the CFM.

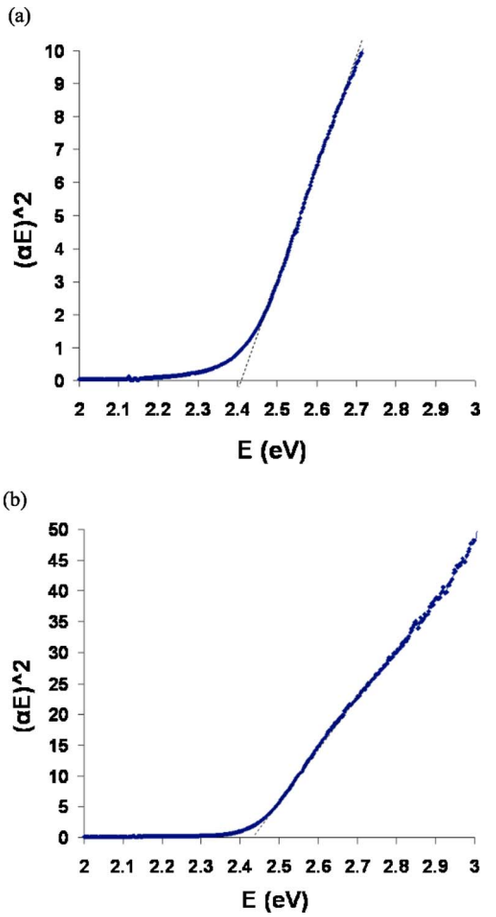

Figure 9. (Color online) Estimated optical bandgaps of as-deposited CdS films deposited by (a) a batch reactor and (b) a CFM.

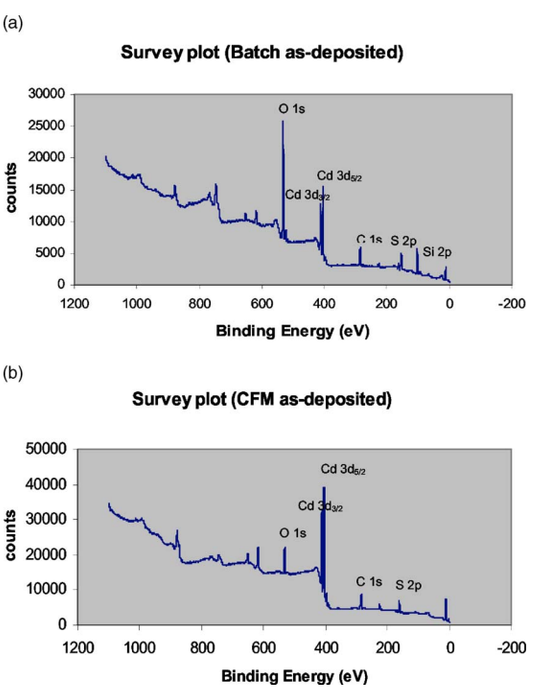

Figure 10. (Color online) XPS spectrums of as-deposited CdS films deposited by (a) a batch reactor and (b) a CFM.

Table I. XPS data for as-deposited CdS films and associated binding energy (eV) peaks (in good agreement with literature values[26,27]).

	Binding energy (eV)		
Photoelectron peak	Batch	CFM	Literature values
Cd $3d_{5/2}$	405.2	405.1	405.2
Cd $3d_{3/2}$	411.9	411.7	411.9
S 2p	161.7	161.4	162.5
O 1s	532	531.6	543.1
C 1s	284.7	284.6	284.2

Using this particle-free flux, we were able to promote the molecule-by-molecule heterogeneous growth mechanism and prevent the particle-by-particle growth. The continuous process has led to more uniform and highly oriented nanocrystalline CdS films with a negligible occurrence of pinholes. This new approach could be adopted for the low-temperature deposition of other compound-semiconductor thin films using a solution-based chemistry with improved control over the processing chemistry.

Acknowledgments

The authors acknowledge Dr. Philip R. Watson and Dr. Cheol-Hee Park from the OSU chemistry department for assistance with AFM and XRD measurements. This work is supported by the National Science Foundation's Process and Reaction Engineering program under a CAREER grant no. CTS-0348723.

Oregon State University assisted in meeting the publication costs of this article.

References

1. C. D. Lokhande, *Mater. Chem. Phys.*, **27**, 1 (1991).
2. D. Lincot, M. Froment, H. Cachet, in *Advances in Electrochemical Science and Engineering*, R. C. Alkire and D. M. Kolb, Editors, Chap. 6, p. 165, Wiley-VCH, New York (1998).
3. R. S. Mane and C. D. Lokhande, *Mater. Chem. Phys.*, **65**, 1 (2000).
4. A. S. Baranski and W. R. Fawcett, *J. Electrochem. Soc.*, **127**, 766 (1980).
5. C. Ghosh and B. P. Verma, *Thin Solid Films*, **60**, 61 (1979).
6. Y. F. Nicolau, *Appl. Surf. Sci.*, **22-23**, 1061 (1985).
7. A. P. Thakoor, B. Raj, D. k. Pandya, and K. L. Chopra, *Thin Solid Films*, **83**, 231 (1981).
8. J. Li, U.S. Pat. 2,002,132,417 (2002).
9. J. Waters, D. Crouch, J. Raftery, and P. O'Brien, *Chem. Mater.*, **16**, 3289 (2004).
10. C.-H. Chang, U.S. Pat. Appl. 11/490,996 (2006); Y.-J. Chang, P. H. Mugdur, A. A. Morrone, S.-Y. Han, S. O. Ryu, T.-J. Lee, and C.-H. Chang, *Electrochem. Solid-State Lett.*, **9**, G174 (2006).
11. Y.-J. Chang, C. L. Munsee, G. S. Herman, J. F. Wager, P. Mugdur, D.-H. Lee, and C.-H. Chang, *Surf. Interface Anal.*, **37**, 398 (2005).
12. C. Voss, Y.-J. Chang, S. Subramanian, S. O. Ryu, T.-J. Lee, and C.-H. Chang, *J. Electrochem. Soc.*, **151**, C655 (2004).
13. P. K. Nair, M. T. S. Nair, V. M. Garcia, O. L. Arenas, Y. Pena, A. Castillo, I. T. Ayala, O. Gomez-Daza, A. Sanchez, J. Campos, et al., *Sol. Energy Mater. Sol. Cells*, **52**, 313 (1998).
14. O. Savadogo, *Sol. Energy Mater. Sol. Cells*, **52**, 361 (1998).
15. P. K. Nair, V. M. Garcia, O. Gomez-Daza, and M. T. S. Nair, *Semicond. Sci. Technol.*, **16**, 855 (2001).
16. H. Löwe, W. Ehrfeld, V. Hessel, T. Richter, and J. Schiewe, in *Proceedings of the 4th International Conference on Microreaction Technology*, IMRET, p. 31 (2000).
17. I. Kaur, D. K. Pandya, and K. L. Chopra, *J. Electrochem. Soc.*, **140**, 943 (1980).
18. R. Ortega-Borges and D. Loncot, *J. Electrochem. Soc.*, **140**, 3464 (1993).
19. M. Kostoglou, N. Andritsos, and A. J. Karabelas, *Ind. Eng. Chem. Res.*, **39**, 3272 (2000).
20. D. Bökenkamp, A. Desai, X. Yang, Y.-C. Tai, E. M. Marzluff, and S. L. Mayo, *Anal. Chem.*, **70**, 232 (1998).
21. Joint Committee for Powder Diffraction Standards, Powder Diffraction File No. 80-0019, 75-0581, 42-1411, and 75-1546, JDCPS International Center for Diffraction Data, Swarthmore, PA (2000).
22. R. Ortega-Borges and D. Lincot, *J. Electrochem. Soc.*, **140**, 3463 (1993).
23. S. M. Sze, *Physics of Semiconductor Devices*, 2nd ed., p. 849, John Wiley, New York (1981).
24. W. J. Danaher, L. E. Lyons, and G. C. Morris, *Sol. Energy Mater.*, **12**, 137 (1985).
25. A. Kylner and M. Wirde, *Jpn. J. Appl. Phys., Part 1* Part 1, **36**, 2167 (1997).
26. M. Stoev and A. Katerski, *J. Mater. Chem.*, **6**, 377 (1996).
27. R. D. Seals, R. Alexander, L. T. Taylor, and J. G. Dillard, *Inorg. Chem.*, **12**, 2486 (1973).